MDPI

Article

Public Decision Policy for Controlling COVID-19 Outbreaks Using Control System Engineering

H. Daniel Patiño [1,*], Julián Pucheta [2], Cristian Rodríguez Rivero [3] and Santiago Tosetti [1]

[1] Instituto de Automática, Faculty of Engineering, Universidad Nacional de San Juan, San Juan J5400ARL, Argentina; stosetti@inaut.unsj.edu.ar
[2] Department of Electrical Engineering, Facultad de Ciencias Exactas, Físicas y Naturales, Universidad Nacional de Córdoba, Córdoba X5016GCA, Argentina; jpucheta@unc.edu.ar
[3] Centre for Engineering Research in Intelligent Sensors and Systems (CeRISS), Cardiff Metropolitan University, Cardiff CF5 2YB, UK; crodriguezrivero@cardiffmet.ac.uk
[*] Correspondence: dpatino@inaut.unsj.edu.ar; Tel.: +54-9264-4992700 or +54-9264-4213303

Abstract: This work is a response to the appeal of various international health organizations and the Automatic Control Community for collaboration in addressing Coronavirus/COVID-19 challenges during the initial stages of the pandemic. Specifically, this study presents scientific evidence supporting the efficacy of three primary non-pharmacological strategies for pandemic mitigation. We propose a control system to aid in formulating a public decision policy aimed at managing the spread of COVID-19 caused by the SARS-CoV-2 virus, commonly known as coronavirus. The primary objective is to prevent overwhelming healthcare systems by averting the saturation of intensive care units (ICUs). In the context of COVID-19, understanding the peak infection rate and its time delay is crucial for preparing healthcare infrastructure and ensuring an adequate supply of intensive care units equipped with automatic ventilators. While it is widely recognized that public policies encompassing confinement and social distancing can flatten the epidemiological curve and provide time to bolster healthcare resources, there is a dearth of studies examining this pivotal issue from the perspective of control system theory. In this study, we introduce a control system founded on three prevailing non-pharmacological tools for epidemic and pandemic mitigation: social distancing, confinement, and population-wide testing and isolation in regions experiencing community transmission. Our analysis and control system design rely on the susceptible–exposed–infected–recovered–deceased (SEIRD) mathematical model, which describes the temporal dynamics of a pandemic, tailored in this research to account for the temporal and spatial characteristics of SARS-CoV-2 behavior. This model incorporates the influence of conducting tests with subsequent population isolation. An On–off control strategy is analyzed, and a proportional–integral–derivative (PID) controller is proposed to generate a sequence of public policy decisions. The proposed control system employs the required number of critical beds and ICUs as feedback signals and compares these with the available bed capacity to generate an error signal, which is utilized as input for the PID controller. The control actions outlined involve five phases of "Social Distancing and Confinement" (SD&C) to be implemented by governmental authorities. Consequently, the control system generates a policy sequence for SD&C, with applications occurring on a weekly or biweekly basis. The simulation results underscore the favorable impact of these three mitigation strategies against the coronavirus, illustrating their efficacy in controlling the outbreak and thereby mitigating the risk of healthcare system collapse.

Keywords: epidemic control; COVID-19; control and modelling; PID control; On–off control; public policy design; healthcare system capacity; social distancing and confinement

1. Introduction

Humanity

Humanity and the scientific community have learned a great deal in just six months since the coronavirus appeared, both in terms of its biology and dynamic behavior. Due to

its high degree of virulence and contagion rate and considering that a potential vaccine may take 10–15 months to be developed, social distancing and confinement, extensive testing, and quarantining of confirmed infected subjects are the most effective tools and actions that public health organisms can apply to control and moderate the COVID-19 outbreak. Taking no action in those directions can, in most cases, increase the number of deceased due to the collapse of the health system and the shortage of ICUs.

It is well known that mathematical models are powerful tools to study and predict the dynamic behavior of processes and systems, both physical and biological [1–3], as well as to assist in decision making and to design automatic control systems [4,5], and cost-effective control for the epidemic system (see [6] and the references therein). In the particular case of the coronavirus pandemic, its dynamic behavior is generally in line with traditional mathematical compartmental models [7–10], such as the susceptible–infected–recovered (SIR) or the SEIR models, that include the number of exposed individuals, which is useful to estimate the spread of the virus, the peak to compute the number of infected individuals, and the number of recovered individuals [11]. Some variants of these have recently been proposed, such as the SIDARTHE model [12,13]. These models are tuned to show the dynamic evolution of the pandemic, the outbreak, the rise time, the peak time and percent overshoot, and the fading stage. These values have been the main scientific-based parameters used to define public policies for mitigating COVID-19 and flattening the peak of the epidemiological curve. Knowledge of the maximum peak and its delay time is important for preparing the healthcare system's infrastructure and obtaining sufficient ICUs with automatic ventilators. The effectiveness of public actions based on social distancing and confinement to flatten the outbreak of the epidemiological curve is well known, and thus it takes time to prepare the healthcare system and increase ICU capacity. However, very few studies have addressed this critical problem from a control system theory point of view, that is, designing a closed-loop feedback control system that can regulate the number of infections that will require care systems and ICUs. Some works along these lines are shown in [13,14]. However, in all approaches, the use of On–off-type control actions is proposed. In this work, a simple control system based on public policy design for controlling the COVID-19 outbreak is proposed to prevent the collapse of healthcare capacity and the saturation of ICUs. The obtained control policy allows for generating a control action sequence of social distancing and confinement that regulates the COVID-19 outbreak, hence maintaining the patients requiring ICUs below a preset threshold, given by the maximum number of intensive care beds available. The main control objective can be stated as follows: Let there be a healthcare system with a finite number of ICUs, and considering the entire pandemic evolution period, it is desired to automatically obtain a control action sequence (scaled social distancing and confinement values) that regulates the COVID-19 outbreak; hence, the infected number (requiring the health system and ICUs) is below a desired set-point. In this way, the collapse of the health system and the saturation of ICUs can be avoided, and so the number of deaths due to a lack of ICU beds can be decreased. The components of the closed-loop control system are a COVID-19 SEIRD model of the process to be controlled [7], which includes the number of deaths (D) due to the infection; public policy as an actuator element; a social distancing and confinement scale as control actions; and, as a feedback signal, the number of infected people demanding hospital assistance and access to ICUs. We assume that the control policy is applied once a week (or once every fortnight), a period generally considered to be a stage or phase in a sequencing social confinement process. An On–off control action is first analyzed, and then a PID controller with anti-windup is proposed [15–19]. The control actions are quantized by amplitude, considering five social distancing and confinement values adapted to the usual public policies that are currently carried out in the pandemic regions. The main advantage of using a PID controller is that it is a model-free controller with robustness to nonlinearities and, in addition, does not require the operator to be familiar with advanced mathematical developments. This paper also includes an estimation of how control actions can influence economic activity. The computational simulation results demonstrate the

practical feasibility of the proposed control system in a real government-decision-making context. The control system presents good performance and robustness to uncertainty, in both the severity of the virus and the model parameters. This robustness is expected owing to the use of a feedback closed-loop system. It also included comparative examples of different public control policies in an open-loop control system, ranging from a weak policy to a very strongly restrictive public policy on confinement and social distancing sequences.

2. Mathematical Modeling of COVID-19 Epidemic

In this section, we describe the COVID-19 epidemic model used to analyze and evaluate the proposed control system. The model used is a SEIRD model, proposed in [7], which includes the number of deaths (D) due to infection, the lack of beds in the care systems, and the ICU capacity. This model computes the infected population and the number of casualties of this epidemic and may be applied to places like the Italian region of Lombardy, where the epidemic started on 25 February 2020. However, it can also be calibrated and adjusted for other regions. In the case of Argentina, the government imposed strict quarantine on 20 March 2020, just two weeks after the first confirmed case appeared. This quick response to the COVID-19 outbreak helped Argentina to control the disease spread compared to other countries in the region that did not take such actions. Over the last three months, different levels or phases of social distancing and confinement have been implemented, ranging from strict quarantine, with no commercial or educational activities allowed, to a more flexible confinement, where some activities except schools and universities are permitted. Deciding when and how to relax isolation policies without collapsing the health system is the subject of this study. Therefore, the differential equations of an epidemic disease process can be represented by a class of graphical mathematical models called compartmental models [20,21]. In this study, the total population is divided into classes, and there are assumptions and laws for individuals to move from one class to another [22,23]. A compartment represents a variable of interest and is assumed to be internally homogeneous, so the individuals inside are indistinguishable. This is also associated with the state variable. For example, given a certain epidemic disease, men and women can be grouped in a single compartment or, depending on the complexity of the model, separated into different compartments. A similar situation can occur with age range, country, and ethnicity. Each compartment interacts with the other compartments through different equations, represented by arrows between the compartments.

At the time when the vaccine was still in development and testing, the isolation of people diagnosed positively and social distancing were the only options to control the spread of SARS-CoV-2.

In this work, an SEIR epidemic disease model is considered [7,10,22–27]. In this model, the total initial population, *N*, is classified into four compartments: the *S(t)*, susceptible; *E(t)*, exposed; *I(t)*, infected/infectious; *R(t)*, recovered; and *D(t)*, dead populations. The relationship between the state variables can be described by the following differential equations:

$$\frac{dS(t)}{d(t)} = \Lambda - \mu S(t) - \frac{\beta}{N}S(t)$$

$$\frac{dE(t)}{dt} = \frac{\beta}{N}S(t)I(t) - (\mu + \varepsilon)E(t)$$

$$\frac{dI(t)}{dt} = \varepsilon E(t) - (\gamma + \mu + \alpha)I(t) \tag{1}$$

$$\frac{dR(t)}{dt} = \gamma I(t) - \mu R(t)$$

$$\frac{dD(t)}{dt} = \alpha I(t)$$

where *N = S + E + I + R*. Equations (1) are subject to the initial conditions *S(0)*, *E(0)*, *I(0)*, *R(0)*, and *D(0)*, and the parameters are defined as: Λ, per-capita birth rate; μ, per-capita

natural death rate; α, virus-induced average fatality rate; β, probability of transmission by contact; ε, rate of progression from exposed to infectious (the reciprocal is the incubation period); γ, recovery rate of infectious individuals (the reciprocal is the infectious period); and N, the total number of alive individuals at time t, with units of *(1/T)*, and *T*: time. The scheme of a typical SEIRD model is illustrated in Figure 1.
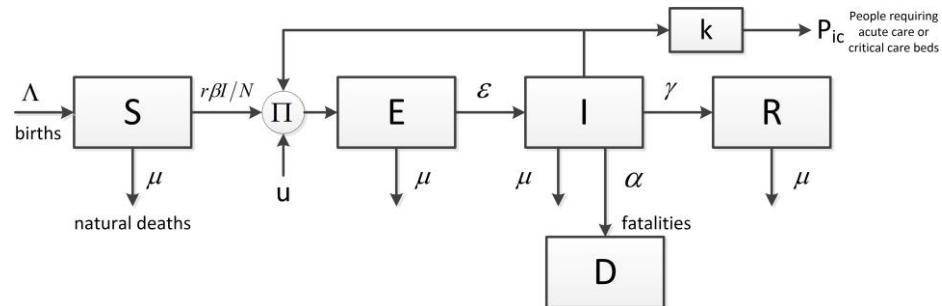
Figure 1. SEIRD epidemic mathematical model.

3. Proposal of a Public Decision Policy for Controlling COVID-19 Outbreaks Based on Control System Engineering

The percentage of total infected people requiring acute care is estimated (approximately 26.7% of all COVID-19 infected per day), which accounts for a given P_{ic}, including both critical care beds and ICUs with mechanical ventilators. The main control objective can be stated as follows: Given a healthcare system capacity (including the number of critical care beds and ICUs required), R_{IUC}, and considering the entire pandemic evolution period described by (1), it is desired to obtain, automatically, a sequence of control actions (scaled social distancing and confinement values for the whole population), *u(t)*, assigning the value β in (1) such that $P_{ic}(t)$ be below a desired set-point, R_{IUC}, given by the maximum health care capacity. Then, the control error can be expressed by

$$e(t) = R_{IUC} - P_{ic}(t) \tag{2}$$

where the period, *t*, is one week or one fortnight, and the design specification, $|R_{IUC} - P_{ic}(t)| < \delta$, $\forall t$, *and* $\delta \in \Re^{+}$, is an arbitrary constant that is as small as possible. The proposed PID *controller law*, in the continuous time domain, is given as

$$u(t) = K\left(K_p e(t) + \frac{1}{T_i} \int_0^t e(\tau)d\tau + T_d \frac{de(t)}{dt} \right) \tag{3}$$

where *u(t)* is the control signal action representing the level of social distancing and confinement, assigning the value β in Equation (1), *e(t)* is the control error, *K* and K_p are the proportional gains, T_i is the integration time, and T_d is the derivative time (lead time). The PID control law comprises three terms, the proportional, integral, and derivative terms. The proportional term, *P*, responds instantly to the feedback control error; the integral term, *I*, improves the steady-state error; and the derivative term, *D*, acts on the transient response of the closed-loop system. For a sample time, T_0, Equation (3) can be transformed into a difference equation via discretization as $t = kT_0$ with $k = 0, 1, 2\ldots$integer. The derivative term is replaced by a first-order difference expression, and the integral term is replaced by a sum. The continuous integration may be approximated by either rectangular or trapezoidal integration, as in [28,29]. In this work, rectangular integration is used, and then Equation (3) can be written as

$$u(k) = K\left\{ K_p e(k) + \frac{T_0}{T_i} \sum_{h=1}^{k} e(h-1) + \frac{T_d}{T_0}[e(k) - e(k-1)] \right\}, \tag{4}$$

where *u(k)* and *e(k)* are the discrete control action and control error, respectively, *k* represents the sampling time variable, and T_0 is the sample time. Equation (4) is a non-recursive control algorithm due to the formation of the sum of all past errors, *e(k)*, which must be stored. However, recursive algorithms are more suitable for programming and are characterized by the calculation of the current manipulated variable, *u(k)*, based on its previous values, *u(k-l)*, and correction terms. To derive a recursive algorithm, *u(k-l)* can be expressed as

$$u(k-1) = K \left\{ K_p e(k-1) + \frac{T_0}{T_i} \sum_{h=1}^{k-1} e(h-1) + \frac{T_d}{T_0} [e(k-1) - e(k-2)] \right\}. \tag{5}$$

Subtracting (5) from (4), the PID control recursive algorithm is given as

$$u_i(k) = u_i(k-1) + a_0 \, e(k) + a_1 \, e(k-1) + a_2 e(k-2), \tag{6}$$

where

$$\begin{aligned} a_0 &= K \left(K_p + \frac{T_0}{T_i} \right) \\ a_1 &= -K \left(K_p + 2\frac{T_d}{T_0} - \frac{T_0}{T_i} \right) \\ a_2 &= K \frac{T_d}{T_0}. \end{aligned} \tag{7}$$

The discrete transfer function, in z-transform, of the difference equation (Equation (7)) can be written following [28,29] as

$$G_{PID}(z) = \frac{U_i(z)}{E(z)} = \frac{a_o + a_1 z^{-1} + a_2 z^{-2}}{1 - z^{-1}} \tag{8}$$

Considering

$$K_i = \frac{T_0}{T_i}, \ \ K_d = \frac{T_d}{T_0}, \ K_i < K_d$$

and combining (7) with (8),

$$G_{PID}(z) = K \left[K_p + K_i \frac{z^{-1}}{1 - z^{-1}} + K_d(1 - z^{-1}) \right] \tag{9}$$

Thus, similar to the continuous-time PID controller, we obtained a separate channel for the *P*, *I*, and *D* terms. Therefore, the single algorithms are

$$\begin{aligned} u_p(k) &= KK_p e(k) \quad\quad P - behaviour \\ u_I(k) &= u_I(k-1) + K \, K_i e(k-1) \ I - behaviour \\ u_d(k) &= K \, K_d(e(k) - e(k-1)) \ \ D - behaviour \end{aligned} \tag{10}$$

Then, the PID algorithm is

$$u_i(k) = u_p(k) + u_I(k) + u_d(k) \tag{11}$$

which is analogous to the continuous-time PID-controller. The choice of T_i, T_d, and K follows the procedure detailed in the literature [15,16], and T_0 is fixed depending on the required dynamics.

In this work, we propose that the signals be quantized in amplitude and time. T_0 is set as the sampling time usually applied in public policy decisions; hence, we choose the period, T_0, to be once a week or every fortnight. We propose five quantized or discretized levels (but they can be chosen arbitrarily, including the On–off control) for the social distancing and confinement policy, *u(k)*, such as

$$u(k) \in \{u_1, u_2, u_3, u_4, u_5\}$$

which can be seen in Table 1. The minimum and maximum values for *u* were taken from a previous work [14], and here, three intermediate values were added.

Table 1. Discretized levels of control action.

Confinement Social Level	Proportion of Baseline Contact Rate	Control Action
Light	70%	$u1 = 2.7$
Weak	50%	$u2 = 2.1$
Medium	30%	$u3 = 1.5$
Strong	20%	$u4 = 0.7$
Extreme	10%	$u5 = 0.2$

The integral action term of the PID algorithm combined with an actuator that becomes saturated can result in undesirable effects. If the control error remains in the integrator, it can saturate the actuator, so the feedback path will be broken because the actuator stays saturated even if the process output changes. To deal with this effect, a PID controller with anti-windup characteristics is proposed, which automatically resets the integrator when the actuator is saturated. The main reason for choosing a PID controller is that it is a model-free controller with a feedback loop that makes it robust to nonlinearities, and in addition, it does not require the operator to be familiar with advanced mathematical developments. Figure 2 shows a block diagram of the PID control algorithm.
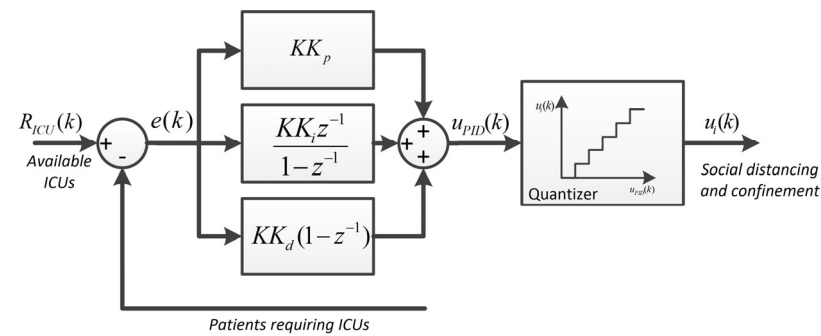
Figure 2. Block diagram of the proposed PID control algorithm for the social distancing and confinement policy.

4. Simulations Analysis and Main Results

In this section, the practical feasibility and performance of the proposed control system are shown by some simulation results. This also proves its good performance and robustness to nonlinearities and uncertainties in the severity of the virus and model parameters.

We use the SEIRD model to compute the infected population and the number of casualties from the COVID-19 epidemic. Let us consider the following parameter basis as a representative example to analyze and design the control system proposed: $N = 20,000$, $\gamma = (1/5)/\text{day}$, $\sigma = 1/7$, and $\alpha = 0.004/\text{day}$. We assume there are five ICU beds available for every 1000 inhabitants [26], i.e., 100, and we take a security threshold, $R_{ICU} = 90$ ICUs. Figure 3 shows the number of individuals in every class of the SEIRD model. Figure 4 shows the cumulative number of dead people *(D)* and the number of deaths per specific day *(D)*. The initial conditions are fixed by the number of exposed people at t = 0, 20,000, with one initial infected person, $I(0) = 1$. The value of the maximum $Ro = 3$, indicating imperfect isolation measures. We can see that the peak of dead individuals per day is reached approximately by day 25 from the beginning of the outbreak. In both figures, social distancing and confinement measures are not considered.
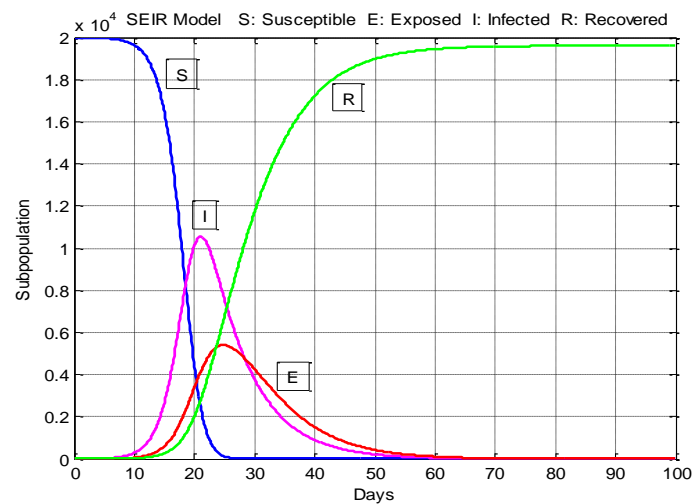
**Figure 3.** Number of humans in the different classes of the SEIRD model.
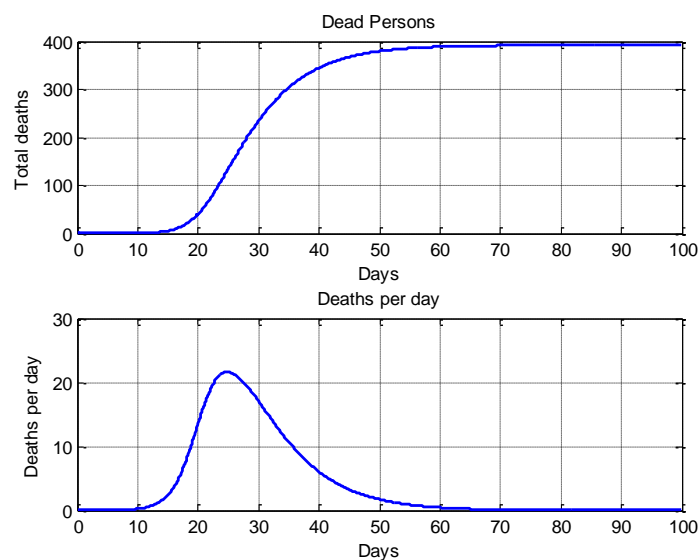
**Figure 4.** Total number of deaths (**top**) and deaths per specific day (**bottom**).

4.1. An Open-Loop Control System Strategy for Social Distancing and Confinement

Firstly, the well-known situation where implementing no social distancing and confinement actions is considered. Economic activity is evaluated in the simulations as a function of social distancing and confinement, considering that only 40% of the population is economically active and assuming that economic activity has a logistic-function-type relationship with social distancing and confinement actions.

Figure 5 shows the highest and longest-lasting peak of a patient whose number is over the available ICU capacity, which represents cases that will likely result in a significantly higher mortality rate. Another extreme case appears when, during the beginning, there are strong social distancing and confinement actions, and after a given time, all restrictions are removed. Figure 6 presents the results in that case, where the peak over the available ICU capacity shifted in time, with the same results as in the previous case. Both in Figures 5 and 6, economic activity is practically not affected when people are moving freely. However, the number of deaths is very significant.
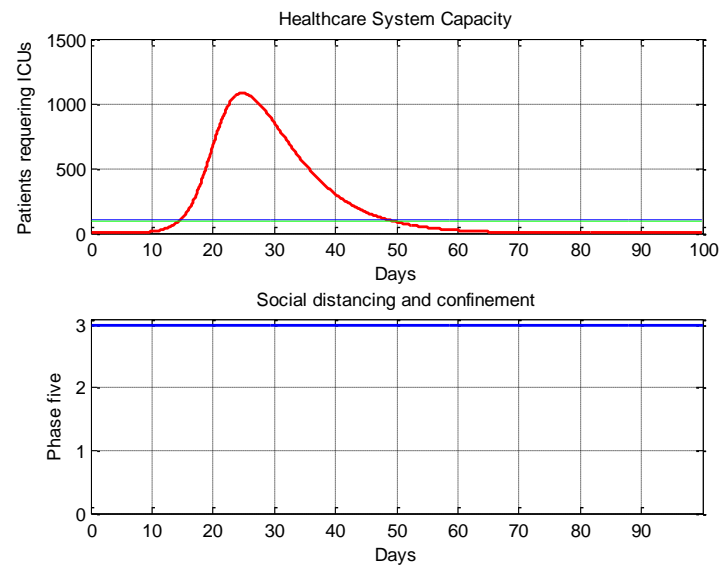
Figure 5. Evolution of patients that need ICUs (**top figure**, red line) and 100 (90 including threshold) available ICU beds (**top figure**, blue and green lines) without any public policy for social distancing and confinement; thus, *u* = 2.7 from Table 1 (**bottom figure**, blue line).
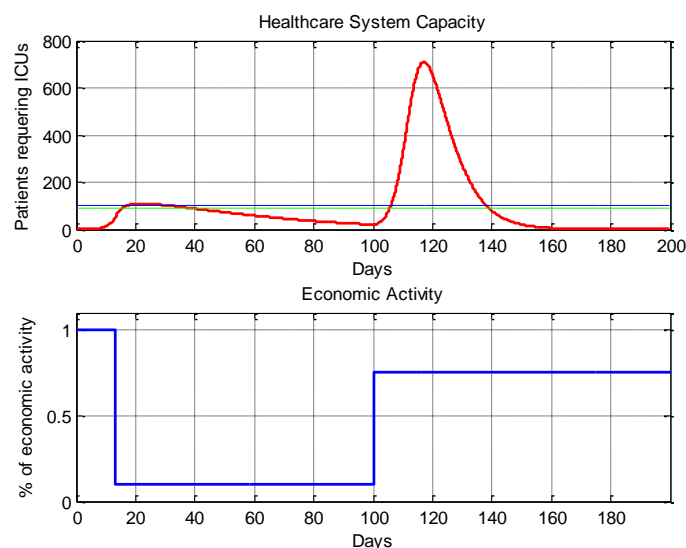
Figure 6. Evolution of patients that need ICUs (**top figure**, red line) and 100 (90 including threshold) available ICU beds (**top figure**, blue and green lines) with strong public policy for social distancing and confinement at the beginning (*u* = 0.2 from Table 1, for day 15 to day 100) and then relaxing all restrictions (*u* = 2 from Table 1, for day 100 to day 200), and the impact on economic activity (**bottom figure**, blue line).

4.2. An On–Off Control System Strategy

One of the most widely used public policies is the On–off control strategy through social distancing and confinement to control the COVID-19 outbreak and avoid health system collapse and ICU bed saturation. The On–off controller is the simplest form of a controller, which switches On when the error between a defined set-point value and feedback signal is positive and switches Off when the error is zero or negative.

The On–off control objective can be formulated as follows: Let the output signal from the controller be *u(t)*, the social distancing and confinement public policy, and the actuating control error signal be *e(t)*, the difference between the set-point and the feedback signal. In two-position control, the signal *u(t)* remains either at a maximum or minimum predefined

value, depending on whether the actuating error signal is positive or negative. The control law is given as

$$u(k) = \begin{cases} U_1 & for\ e(k) \geq 0 \\ U_2 & for\ e(k) < 0 \end{cases}$$
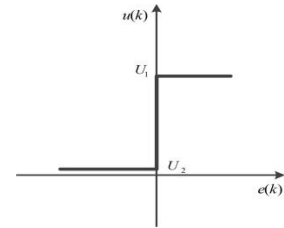
where U_2 is the minimum distance and confinement social action, and U_1 is the strongest action. This controller is simple; however, when the system operates close to the set-point, an undesirable oscillation (chattering) is generated. To avoid chattering, practical On–off controllers usually have a dead zone around the set point,

$$u(k) = \begin{cases} U_1 & for\ e(k) > b_n \\ 0 & for\ |e(k)| \leq b_m \\ U_2 & for\ e(k) < -b_m \end{cases}$$
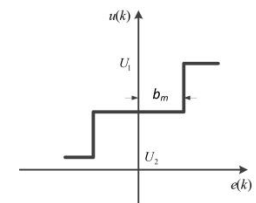
or even hysteresis,

$$u(k) = \begin{cases} U_1 & for\ e(k) \geq b_m \\ U_2 & for\ e(k) < -b_m \end{cases}$$
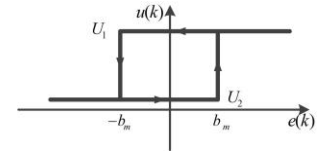
Figure 7 shows the block diagrams for two-position or On–off controllers.
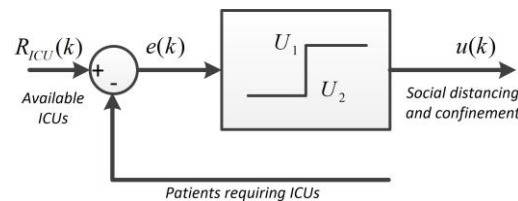
Figure 7. Block diagram of an On–Off controller, and with differential gap type.

The On–off controller is often called a bang–bang controller or a two-step controller since the manipulated variable output of the controller rapidly switches between On and Off with no intermediate state. This control type applied to the COVID-19 outbreak works as follows: when the number of new patients requiring acute care or ICUs is below a threshold (set point), the control action is low confinement and social distancing, whereas when new patients exceed that threshold, then the social distancing and confinement action is strong. Economic activity is evaluated in the simulations as a function of social distancing and confinement, considering that only 40% of the population is economically active and assuming the economic activity has a logistic-function-type relationship with the social distancing and confinement actions. Figure 8 shows an On–off public policy of social distancing and confinement, considering a sampling time of $T_0 = 1$ day, with a good performance, but it is impractical. This type of controller improves its performance when the sampling period decreases. In Figure 9, a flattening of the infected people curve can be seen due to the application of the On–off control system. Figures 10 and 11 show this for $T_0 = 3$ days and $T_0 = 15$ days, respectively.
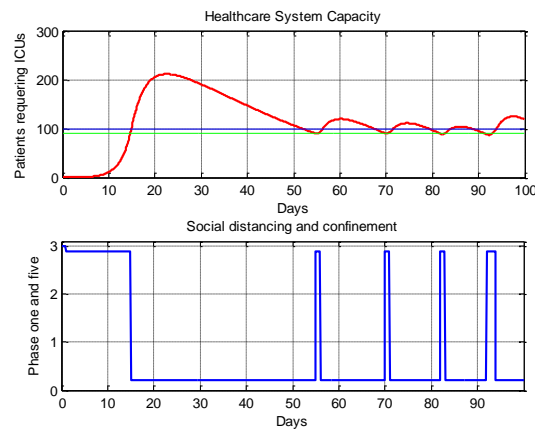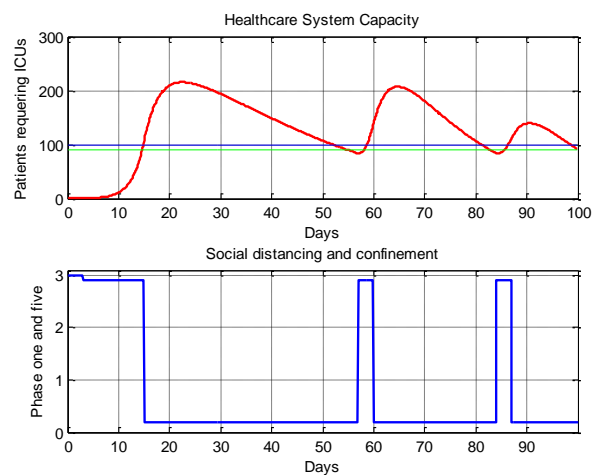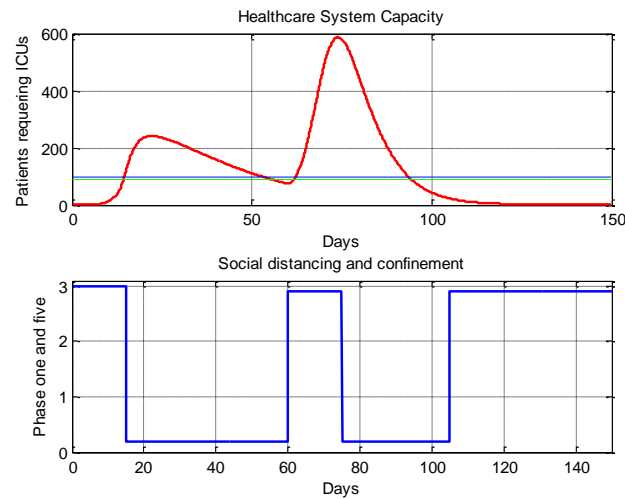
Figure 8. Evolution of patients that need ICUs (**top figure**, red line) and 100 (90 including threshold) available ICU beds (**top figure**, blue and green lines) using On–off control strategy, *u(t)*, with the sampling time $T_0 = 1$ day (**bottom figure**, blue lines) and *u(t)* assigned to β in Equation (1).
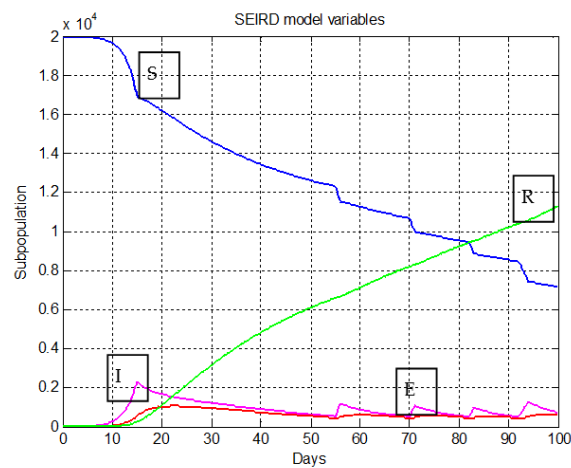
Figure 9. Evolution of SEIRD variables, where each individual are either susceptible (S) to the disease, exposed (E) to the disease, infected (I) by the disease, and recovered (R) or died (D) from the disease. Flattening of the infected curve (fuchsia line) due to On–off control system using a sampling time $T_0 = 1$ day.

Figure 10. Evolution of patients that need ICUs (**top figure**, red line) and 100 (90 including threshold) available ICU beds (**top figure**, blue and green lines) using an On–off control strategy *u(t)* with a sampling time $T_0 = 3$ days (**bottom figure**, blue line) and *u(t)* assigned to β in Equation (1).

Figure 11. Evolution of patients that need ICUs (**top figure**, red line) and 100 (90 including threshold) available ICU beds (**top figure**, blue and green lines) using an On–off control strategy with a sampling time T_0 = 15 days (**bottom figure**, blue line) and *u(t)* assigned to β in Equation (1).

4.3. Main Results for the Proposed PID Control System

The PID controller is the most intuitive and practical feedback control system widely used in engineering [27,30] and other technical fields since its introduction in a paper by Nicolas Minorsky in 1922 [31] and the Taylor Instrument Company in 1936 in the industry field. The main objective of the proposed PID controller is to regulate the COVID-19 outbreak to avoid the collapse of the health system and the saturation of the ICU beds. Figure 12 shows a block diagram of the proposed PID-based control system for controlling the COVID-19 outbreak. The control error is defined as the difference between the desired set point, *RIUC*, given by the maximum health care capacity (including the number of critical care bed and ICUs required), and the number of patients requiring ICUs, *PIC*. The main objective of the PID controller is to make the control error as small as possible, such as $|R_{IUC} - P_{IC}| \leq \delta$, $\delta \in \mathbb{R}^+$. Then, the control action is quantized by amplitude into five levels of social distancing and confinement, detailed in Table 1, and applied by public authority. The loop is closed by the feedback signal, *PIC*, which is the number of patients requiring ICUs.
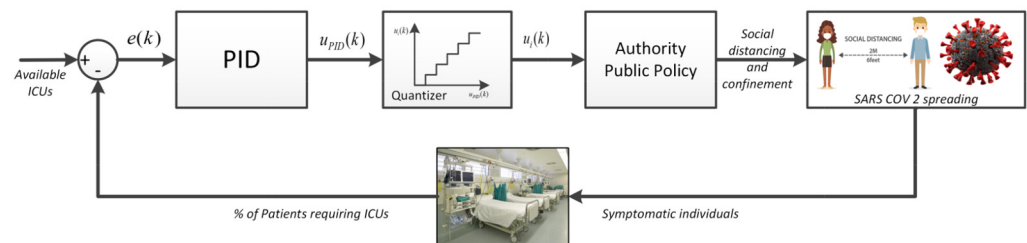

Figure 12. Block diagram of the proposed PID-based control system as a public authority policy.

A PID controller was chosen because it has a model-free design, is robust to nonlinearity, is very simple, and has an easy-to-understand operation. A computational simulation study was carried out using the COVID-19 SEIRD epidemic model presented in Section 2, considering that 6.5% of patients require an ICU bed with ventilation [26]. The set point is R_{ICU} = 90 ICUs. The PID parameters were tuned, resulting in K_p = 0.95, Ki = 0.012/6.5, and K_d = 7.5. Figure 13 shows the PID performance for a sampling time of T_0 = 7 days. Figure 14 shows the flattering of the infected individuals curve due to feedback PID control. Figure 15 presents the same controller parameters but for T_0 = 3 days, showing better performance, as expected. The robustness of the PID controller to uncertainty in the model parameters is proven by considering an uncertainty of 10% in the SEIRD model parameters.

Figure 16 shows the above-mentioned case. In Figure 17, we show the performance of the proposed control system considering that people's behavior is such that it does not obey the suggested actions of social distancing and confinement, estimated at 35% of people in each *u(k)*. The predictive PID controller [28] operation can be seen when the feedback signal $\Delta P_{IC} = P_{IC}(k) - P_{IC}(k-1)$ is considered, which improves the performance. Working in a heuristic way with a value of $\Delta P_{IC} = 0.5(P_{IC}(k) - P_{IC}(k-1))$, we obtain a pattern profile, in which for a phase 2 period of approximately 80 days, very good performance is achieved; see Figures 18 and 19, which use ΔP_{IC} and $\Delta P_{IC}/2$, respectively.
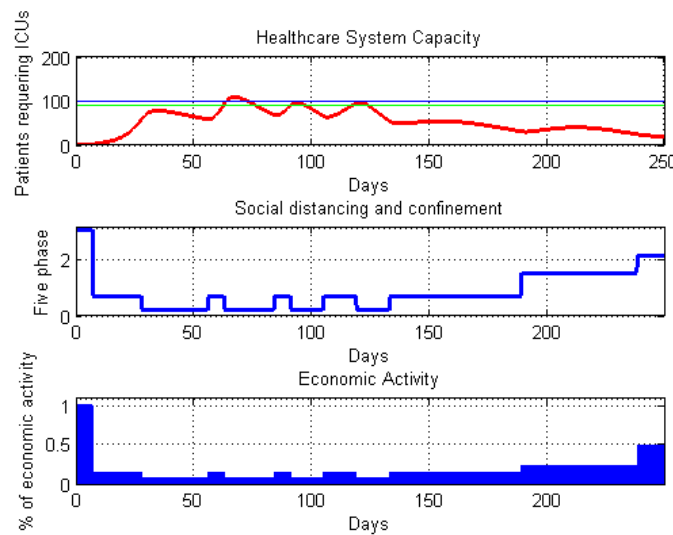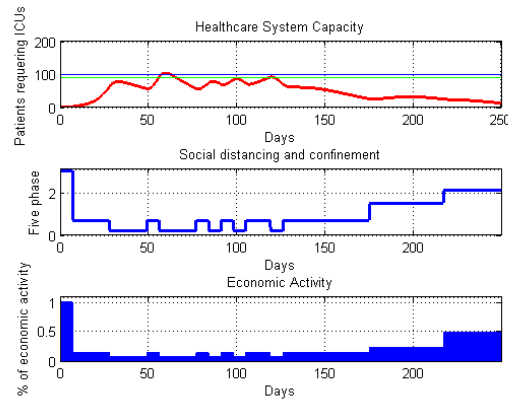

Figure 13. PID controller with a sampling time of T_0 = 7 days. Evolution of patients that need ICUs (**top figure**, red line) and 100 (90 including threshold) available ICU beds (**top figure**, blue and green lines). Trajectory of *u(t)* updated every 7 days (**middle figure**, blue line) with *u(t)* assigned to *β* in Equation (1). The economic activity is detailed in the **bottom figure** (blue line), ranging from 0 (closed) to 100% (normal).
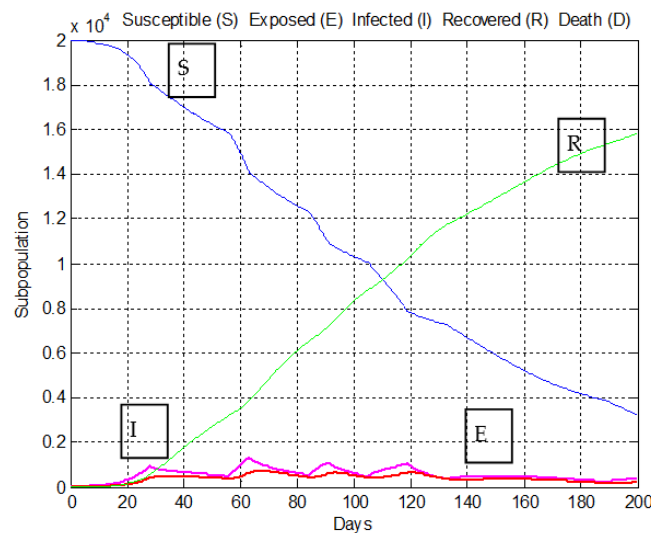

**Figure 14.** Flattening of the infected curve (fuchsia line) due to PID control system.
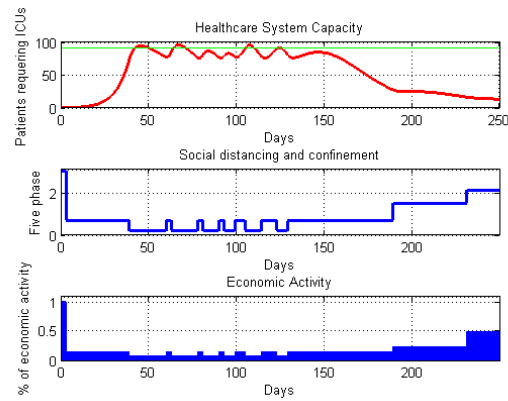
Figure 15. PID controller with a sampling time of T_0 = 3 days. Evolution of patients that need ICUs (**top figure**, red line) and 100 (90 including threshold) available ICU beds (**top figure**, blue and green lines). Trajectory of *u(t)* updated every 3 days (**middle figure**, blue line) with *u(t)* assigned to β in Equation (1). The economic activity is detailed in the **bottom figure**, ranging from 0 (closed) to 100% (normal).


Figure 16. PID controller performance considering an uncertainty of 10% in the SEIRD model parameters, and with a sampling time of T_0 = 7 days. Evolution of patients that need ICUs (**top figure**, red line) and available ICU beds (**top figure**, blue-cyan line). Trajectory of *u(t)* updated every 7 days (**middle figure**, blue line) with *u(t)* assigned to β in Equation (1). The economic activity is detailed in the **bottom figure**, ranging from 0 (closed) to 100% (normal).
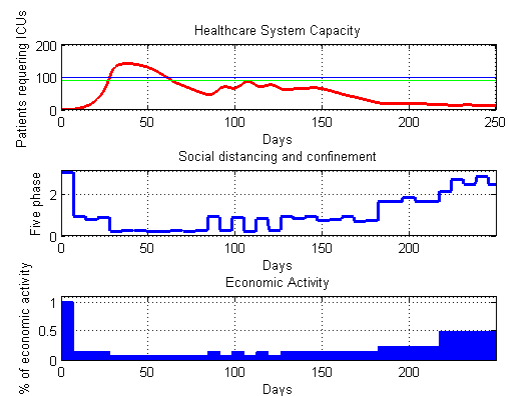
Figure 17. PID controller performance considering 35% of people do not abide by the social distancing and confinement actions suggested by the PID control system. T_0 = 7 days. Evolution of patients that need ICUs (**top figure**, red line) and 100 (90 including threshold) available ICU beds (**top figure**, blue and green lines). Trajectory of *u(t)* updated every 7 days (**middle figure**, blue line) with *u(t)* assigned to β in Equation (1). The economic activity is detailed in the **bottom figure**, ranging from 0 (closed) to 100% (normal).
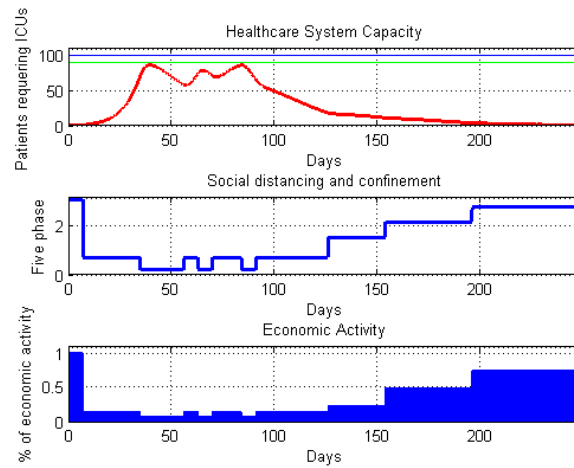
Figure 18. PID controller with a sampling time of T_0 = 7 days and feedback signal, $\Delta PIC(k)$, for improving performance. Evolution of patients that need ICUs (**top figure**, red line) and 100 (90 including threshold) available ICU beds (**top figure**, blue and green lines). Trajectory of $u(t)$ updated every 7 days (**middle figure**, blue line) with $u(t)$ assigned to β in Equation (1). The economic activity is detailed in the **bottom figure**, ranging from 0 (closed) to 100% (normal).
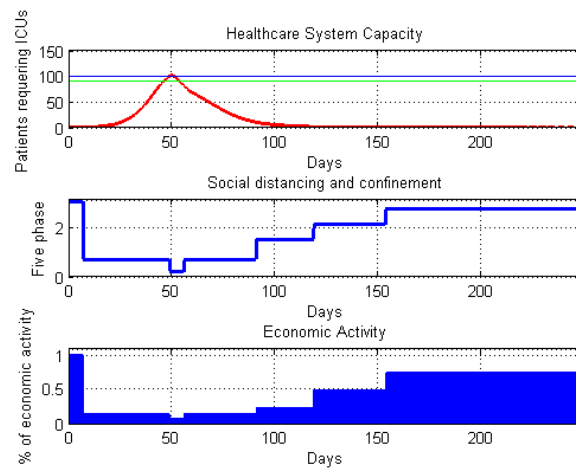
Figure 19. PID controller with a sampling time of T_0 = 7 days and $\Delta PIC(k)/2$. Evolution of patients that need ICUs (**top figure**, red line) and 100 (90 including threshold) available ICU beds (**top figure**, blue and green lines). Trajectory of $u(t)$ updated every 7 days (**middle figure**, blue line) with $u(t)$ assigned to *β* in Equation (1). The economic activity is detailed in the **bottom figure** (blue line), ranging from 0 (closed) to 100% (normal).

These simulation results show the practical feasibility, good performance, and robustness of the proposed approach and show the pattern of the social distancing and confinement sequence profile, both in the corresponding phase and in its duration over time.

4.4. Modification of the SEIRD Model, Including the Testing of Asymptomatic and Presymptomatic Subjects

In these computational simulations, a modification of the SEIRD epidemiological model, Equation (1), is considered, in which, in addition to representing susceptible (*S(t)*), exposed (*E(t)*), infected (*I(t)*), recovered (*R(t)*), and deceased (*D(t)*) subjects, the testing of asymptomatic and pre-symptomatic subjects is incorporated, as in [26,31].

Considering a population of size *N* divided into six compartments, *S* susceptible individuals; *E* exposed but not yet contagious individuals; I_a, asymptomatic individuals with no symptoms or mild symptoms; *R*, recovered individuals; *D*, deceased individuals, and I_p, pre-symptomatic individuals who eventually develop symptoms, and the constraint

$N = S + E + I_a + R + D + I_p$, a dynamical model can be described by the following set of differential equations

$$\frac{dS(t)}{d(t)} = -\frac{\beta_a}{N}(\mu(t)S(t)I_a(t)) - \frac{\beta_p}{N}(\mu(t)S(t)I_p(t))$$

$$\frac{dE(t)}{dt} = \frac{\beta_a}{N}\mu(t)S(t)I_a(t) - \sigma E(t) + \frac{\beta_p}{N}(\mu(t)S(t)I_p)$$

$$\frac{dI_a(t)}{dt} = \alpha\sigma E(t) - (\gamma_a + \rho(t)v_a)I_a(t)$$

$$\frac{dR(t)}{dt} = \gamma_c I_p(t)$$

$$\frac{dD(t)}{dt} = \alpha I_a(t)$$

$$\frac{I_p(t)}{dt} = (1-\alpha)\sigma E(t) - \gamma_p I_p(t) - \rho(t)v_p I_p(t)$$

where $\mu(t)$ is the intervention factor for social distancing and confinement; $\rho(t)$ is the intervention factor for testing and isolation; α is the portion of asymptomatic carriers; β_a is the asymptomatic portion; β_p is the portion of pre-symptomatic individuals; σ is the rate of exposure to infected people; γ_a is the transition rate from asymptomatic to recovered or hospitalized patients; γ_p is the transition rate from pre-symptomatic to recovered or hospitalized; and v_a, v_p are the probabilities of detecting asymptomatic carriers and symptomatic carriers, respectively. In these experiments, the proposed control system employs the PID controller tuned with the following range of gains: $K = 0.01 - 0.009$, $K_p = 1.65$, $K_i = 0.012/6.5$, and $K_d = 5 - 150$.

Figure 20 shows the evolution of the controlled variable, $P_{IC}(t)$, for a sampling period of $T_0 = 7$ days without testing and isolation, and it can be observed that there is no saturation of the health system. Figure 21 shows how the curve of infected people, and therefore the number of patients who require medical attention, is flattened due to the automatic generation of the corresponding sequence of phases. Figure 22 shows the positive impact of using both the application of the phases generated by the controller and the isolation test. Note that by incorporating the strategy of testing with isolation, the mobility of the population can increase, allowing more opportunities for economic and social activities.
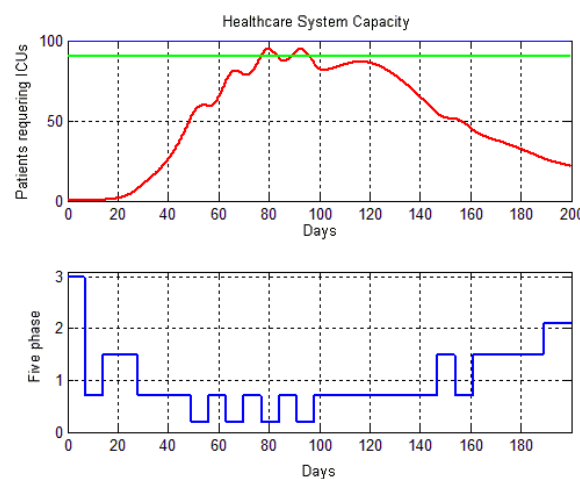
Figure 20. Response of the proposed control system without testing with isolation. Evolution of patients that need ICUs (**top figure**, red line) and 100 (90 including threshold) available ICU beds (**top figure**, blue and green lines). Trajectory of $u(t)$ updated every 7 days (**below figure**, blue line) with $u(t)$ assigned to β in Equation (1).
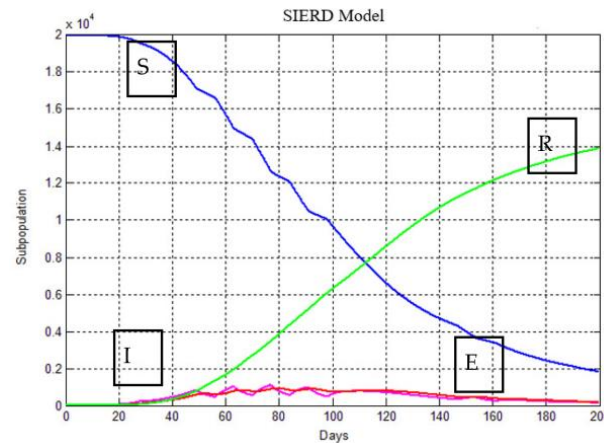
Figure 21. Evolution of SEIRD variables, where each individual is either susceptible (S) to the disease, exposed (E) to the disease, infected (I) by the disease, and recovered (R) or died (D) from the disease. Flattening of the infected curve (fuchsia line) due to an On−off control system with a sampling time interval T_0 = 1 day.
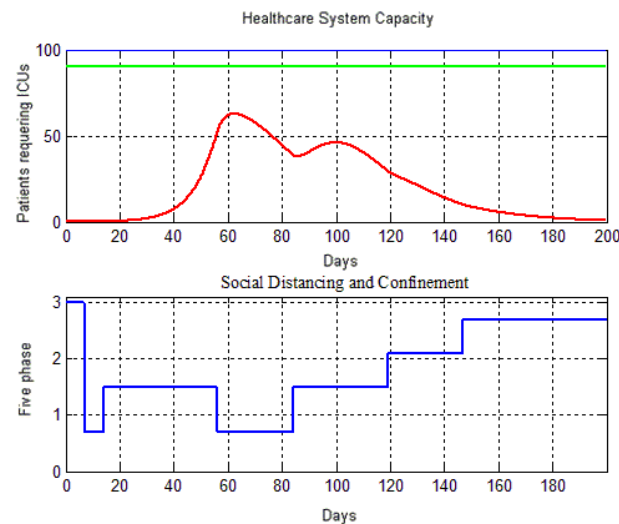
Figure 22. Positive impact of social distancing and confinement with all mitigation tools, testing, and mass isolation of the population. Evolution of patients that need ICUs (**top figure**, red line) and 100 (90 including threshold) available ICU beds (**top figure**, blue and green lines). Trajectory of *u(t)* updated every 7 days (**below figure**, blue line) with *u(t)* assigned to β in Equation (1).

Further simulations were carried out, in which the robust behavior of the PID controller was obtained in the face of uncertainties in the model, considering a 10% error. Another situation experienced is the case in which 35% of the population does not obey the directives and orders of the government authority regarding social distancing and confinement.

It has been found that the performance of the control system can be improved by adding a predictive control action, considering, as a feedback signal, $\Delta P_{IC}(k) = 0.5\left(P_{IC}(k) - P_{IC}(k-1)\right)$. Figure 23 shows the system's response to the proposed modification.
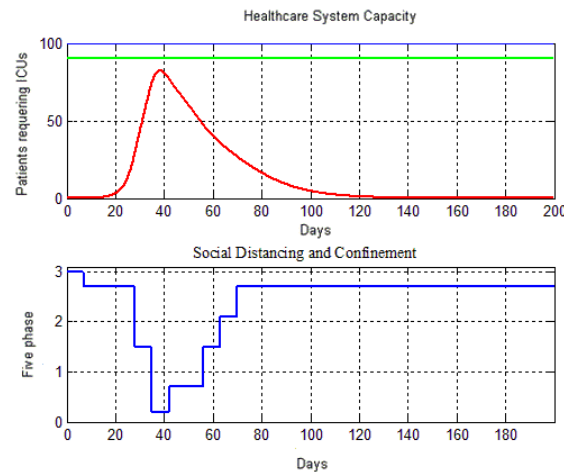
Figure 23. Response to predictive PID. No testing. Evolution of patients that need ICUs (**top figure**, red line) and 100 (90 including threshold) available ICU beds (**top figure**, blue and green lines). Trajectory of *u(t)* updated every 7 days (**below figure**, blue line) with *u(t)* assigned to *β* in Equation (1).

5. Conclusions

This work was in response to the requirements of the IFAC, IEEE, the World Health Organization, and other institutions at the beginning of 2020, with the main objective of contributing to the fight against COVID-19 and future pandemics from a systems and control theory approach. There are many influences of the outbreak that were not considered in the present approach, which are important in an overall strategy towards the spread of COVID-19 and flattening the epidemiological curve, e.g., extensive testing, tracking infections, and quarantining confirmed infected subjects. It has been proven that the proper and correct use of a high-quality mask is equivalent to the confinement of people. However, it is well known that controlling the infection rate is one of the key actions, and hence, this work contributes towards that direction.

In this paper, we have used social distancing, confinement, and testing with the isolation of infected individuals, including pre- and asymptomatic detection, as a public policy to fight against the COVID-19 outbreak, mainly to avoid the saturation of the health system and ICU capacity. An approach that tries to regulate the COVID-19 outbreak based on a feedback PID control system was presented, resulting in a simple and robust control strategy for generating a sequence of social distancing and confinement as a public policy involving the whole population. A PID controller was chosen mainly because it is a model-free controller, it is very intuitive and practical, and it does not require the operator to be familiar with advanced mathematical developments. The main objective of the proposed PID controller is to regulate the COVID-19 outbreak to avoid the collapse of the sanitary system and the saturation of ICU beds. In this way, the feedback control strategy proposed can help public health authorities in their efforts to contain the virus, mainly in the outbreak phase. We have used a COVID-19 SEIRD model to analyze and design an On–off control strategy and the PID anti-windup controller proposed. This strategy uses the health system and ICU capacity as a feedback signal measure for determining when physical and social distancing and confinement should be tightened up and when they should be relaxed. The control system generates a sequence of five possible levels of social distancing and confinement actions. These are useful measures for the decisions of policymakers. To show the practical feasibility and performance of the PID-based control algorithm, as well as its stability and robustness properties, simulation studies were carried out for the COVID-19 SEIRD mathematical model. These simulation results also produce a social distancing and confinement sequence profile, both in the corresponding phase and in its duration over time, which can be helpful for public social distancing and confinement policies. Scientific evidence has been given for the effectiveness of the three main non-pharmacological pandemic mitigation tools.

The directions for future investigation will be oriented toward the optimization and adaptive issues of the PID-based control structures, including their impact on economic activity by using suitable metrics and indexes and including in the mathematical model extensive testing to apply to the quarantining of confirmed infected subjects.

This research supports and validates the strategies of many health groups carried out in many countries in the field of control systems engineering. It can also be very helpful and useful for public authorities in their decision making, especially in those places and countries where the virus is not yet circulating or is in its initial stage of circulation. We hope this paper inspires further investigations into the control system for fighting the COVID-19 outbreak or other possible pandemics in the future.

References

1.   Rutherford, A. *Mathematical Modelling Techniques*; Dover: New York, NY, USA, 1994.
2.   Bender, E.A. *An Introduction to Mathematical Modeling*; Dover: New York, NY, USA, 2000.
3.   Gershenfeld, N. *The Nature of Mathematical Modeling*; Cambridge University Press: Cambridge, UK, 1998.
4.   Ogata, K. *Modern Control Engineering*, 5th ed.; Prentice Hall: Upper Saddle River, NJ, USA, 2010.
5.   Kuo, B. *Automatic Control Systems*, 9th ed.; Prentice Hall: Upper Saddle River, NJ, USA, 2014.
6.   Bandekar, S.R.; Ghosh, M.; Bi, K. Impact of high-risk and low-risk population on COVID-19 dynamics considering antimicrobial resistance and control strategies. *Eur. Phys. J. Plus.* **2023**, *138*, 697. [CrossRef]
7.   Carcione, J.M.; Santos, J.E.; Bagaini, C.; Ba, J. A simulation of a COVID-19 epidemic based on a deterministic SEIR model. *Front. Public Health* **2020**, *8*, 230. [CrossRef] [PubMed]
8.   Brauer, F. Compartmental Models in Epidemiology. In *Mathematical Epidemiology*; Chapter in Lecture Notes in Mathematics; Springer: Berlin/Heidelberg, Germany, 2008. [CrossRef]
9.   Willis, M.J.; Díaz, V.H.G.; Prado-Rubio, O.A.; von Stosch, M. Insights into the dynamics and control of COVID-19 infection rates. *J. Chaos Solitons Fractal* **2020**, *138*, 109937. [CrossRef] [PubMed]
10. Sameni, R. Mathematical Modeling of Epidemic Diseases; A Case Study of the COVID-19 Coronavirus. In *Quantitative Biology, Populations and Evolution*; Draf Paper; Cornel University: Ithaca, NY, USA, 2020.
11. Ferguson, N.; Laydon, D.; Nedjati Gilani, G.; Imai, N.; Ainslie, K.; Baguelin, M.; Bhatia, S.; Boonyasiri, A.; Cucunuba Perez, Z.; Cuomo-Dannenburg, G.; et al. *Impact of Non-Pharmaceutical Interventions (NPIs) to Reduce COVID-19 Mortality and Healthcare Demand*; Imperial College COVID-19 Response Team: London, UK, 2020. [CrossRef]
12. Giordano, G.; Blanchini, F.; Bruno, R.; Colaneri, P.; Di Filippo, A.; Di Matteo, A.; Colaneri, M. Modelling the COVID-19 epidemic and implementation of population-wide interventions in Italy. *Nat. Med.* **2020**, *26*, 855–860. [CrossRef] [PubMed]
13. CTsay, C.; Lejarza, F.; Stadtherr, M.A.; Baldea, M. Modeling, state estimation, and optimal control for the US COVID-19 outbreak. *Sci. Rep.* **2020**, *10*, 10711. [CrossRef]

14. Stewart, G.; van Heusden, K.; Dumont, G.A. Coronavirus: Policy Design for Stable Population Recovers: Using Feedback to Maximize Population Recovery Rate While Respecting Healthcare Capacity. IEEE Spectrum, 17 April 2020. Available online: https://spectrum.ieee.org/biomedical/diagnostics/how-control-theory-can-help-control-covid19 (accessed on 22 December 2023).

15. Åström, K.J.; Hägglund, T. *Advanced PID Control*; International Society of Automation: Durham, NC, USA, 2006.

16. Åström, K.J.; Hägglund, T. *Control PID Avanzado*; Pearson Educación, S.A.: Madrid, Spain, 2009.

17. Cvejn, J. PID control of FOPDT plants with dominant dead time based on the modulus optimum criterion. *Arch. Control. Sci.* **2016**, *26*, 5–17. [CrossRef]

18. Wang, C.; Li, D. Decentralized PID Controllers Based on Probabilistic Robustness. *J. Dyn. Syst. Meas. Control* **2011**, *133*, 61015. [CrossRef]

19. Knospe, C. PID Control. *IEEE Control. Syst. Mag.* **2006**, *26*, 30–31. [CrossRef]

20. Chitnis, N. Introduction to SEIR Models. In *Workshop on Mathematical Models of Climate Variability, Environmental Change and Infectious Diseases*; Department of Epidemiology and Public Health Systems Research and Dynamical Modelling: Trieste, Italy, 2017.

21. Brauer, F. *Chapter 2 Compartmental Models in Epidemiology*; Department of Mathematics, University of British Columbia: Vancouver, BC, Canada, 1984.

22. Brauer, F.; Castillo-Chavez, C. *Mathematical Models in Population Biology and Epidemiology*; Springer: Berlin/Heidelberg, Germany, 2012; Volume 2.

23. Diekmann, O.; Heesterbeek, H.; Britton, T. *Mathematical Tools for Understanding Infectious Disease Dynamics*; Princeton University Press: Princeton, NJ, USA, 2012; Volume 7.

24. Das, A.; Dhar, A.; Goyal, S.; Kundu, A. COVID-19: Analysis of a modified SEIR model, a comparison of different intervention strategies and projections for India. *Prepr. Serv. Health Sci.* **2020**, preprints. [CrossRef]

25. Al-Sheikh, S.A. Modeling and Analysis of an SEIR Epidemic Model with a Limited Resource for Treatment. *Glob. J. Sci. Front. Res. Math. Decis. Sci.* **2012**, *12*, 56–66.

26. Giannakeas, V.; Bhatia, D.; Warkentin, M.T.; Bogoch, I.; Stall, N.M. Estimating the Maximum Capacity of COVID-19 Cases Manageable per Day Given a Health Care System's Constrained Resources. *Am. Coll. Physicians J. Ann. Intern. Med.* **2020**, *173*, 407–410. [CrossRef] [PubMed]

27. Hadi, M.A.; Ali, H.I. Control of COVID-19 system using a novel nonlinear robust control algorithm. *Biomed. Signal Process Control.* **2021**, *64*, 102317. [CrossRef] [PubMed]

28. Kuchen, B.; Carelli, R. *Control Digital Directo*; School of Engineering, Universidad Nacional de San Juan: San Juan, Argentina, 2010.

29. Isermann, R. *Digital Control System*; Springer-Verlag: Berlin/Heidelberg, Germany, 1989; Volume 1.

30. Arasteh, H.; Badi, A. A Study on Control of Novel corona-virus (2019-nCoV) Disease Process by Using PID Controller. *medrxiv* **2020**, *23*, 1–9. [CrossRef]

31. Minorsky, N. Directional stability of automatically steered bodies. *J. Am. Soc. Nav. Eng.* **1922**, *34*, 280–309. [CrossRef]